Journal of Computer-Aided Molecular Design (2006) 20: 67–81
DOI 10.1007/s10822-006-9037-3

Comparison of a homology model and the crystallographic structure of human 11β-hydroxysteroid dehydrogenase type 1 (11βHSD1) in a structure-based identification of inhibitors

Laurence Miguet[a], Ziding Zhang[b], Maryse Barbier[a] & Martin G. Grigorov[a,*]
[a]*BioAnalytical Science, Nestlé Research Center, Nestec Ltd, CH-1000, Lausanne 26, Switzerland;* [b]*Bioinformatics Center, College of Biological Science, China Agricultural University, 100094, Beijing, China*

Received 26 September 2005; accepted 23 January 2006

Key words: 11β-Hydroxysteroid dehydrogenase type 1, diabetes type 2, homology modeling, inhibitor, molecular docking

Summary

Human 11β-hydroxysteroid dehydrogenase type 1 (11βHSD1) catalyzes the interconversion of cortisone into active cortisol. 11βHSD1 inhibition is a tempting target for the treatment of a host of human disorders that might benefit from blockade of glucocorticoid action, such as obesity, metabolic syndrome, and diabetes type 2. Here, we report an *in silico* screening study aimed at identifying new selective inhibitors of human 11βHSD1 enzyme. In the first step, homology modeling was employed to build the 3D structure of 11βHSD1. Further, molecular docking was used to validate the predicted model by showing that it was able to discriminate between known 11βHSD1 inhibitors or substrates and non-inhibitors. The homology model was found to reproduce closely the crystal structure that became publicly available in the final stages of this work. Finally, we carried out structure-based virtual screening experiments on both the homology model and the crystallographic structure with a database of 114'000 natural molecules. Among these, 15 molecules were consistently selected as inhibitors based on both the model and crystal structures of the enzyme, implying a good quality for the homology model. Among these putative 11βHSD1 inhibitors, two were flavonone derivatives that have already been shown to be potent inhibitors of the enzyme.

Introduction

Due to excessive caloric intake, improper nutrition and inadequate physical activity, the incidence of obesity has increased dramatically throughout the world, most notably over the last two decades [1]. The World Health Organization has coined a new word, globesity, to describe this situation. In the United States, 31% of adults are obese, with a body mass index (BMI, in kg/m^2, calculated as body weight divided by height squared) greater than 30. (http://www.cdc.gov/nchs/products/pubs/pubd/hestats/obese/obse99.htm) The rest of the western world is not far behind, and developing countries are following a similar trajectory. Obesity is frequently associated with the highly prevalent metabolic syndrome (glucose intolerance, insulin resistance, type II diabetes, abdominal obesity, dyslipidemia, hypertension, congestive heart failure) [2]. This common metabolic syndrome resembles the rare Cushing's syndrome characterized by a glucocorticoid excess.

*To whom correspondence should be addressed. Tel.: +41-21-785 8939; Fax: +41-21-785 9486; E-mail: martin.grigorov@rdls.nestle.com

Glucocorticoid action is, in part, regulated at a pre-receptor level by the enzyme 11-β hydroxysteroid dehydrogenase (11βHSD) that interconverts hormonally inactive cortisone into active cortisol in humans. Two 11βHSD isoforms regulate glucocorticoid access to intracellular receptors. 11βHSD type 1 (11βHSD1) is highly expressed in key metabolic tissues including liver, adipose tissue, and the central nervous system. In these tissues, 11βHSD1 uses NADPH to reduce cortisone to cortisol [3, 4]. Sharing only 14% sequence identity with 11βHSD1, 11βHSD type 2 (11βHSD2) is found mainly in aldosterone-selective tissues. 11βHSD2 acts as a NAD^+-dependent dehydrogenase oxidizing cortisol to cortisone, thereby preventing illicit activation of the mineralocorticoid receptor [5].

In obesity, plasma cortisol levels are not elevated, but 11βHSD1 activity is locally elevated in adipose tissue but not in liver [6], this has stemmed from recognition of the role of 11βHSD1 in adipose tissue. Mice with adipose-specific 11βHSD1 overexpression exhibit glucose intolerance, insulin resistance and visceral obesity [7]. Conversely, pharmacologic inhibition or transgenic disruption of 11βHSD1 attenuates glucocorticoid action and increases insulin sensitivity [8, 9]. 11βHSD1 inhibition shows considerable promise as a therapeutic target in the metabolic syndrome.

Containing 292 amino acids, 11βHSD1 belongs to the superfamily of short-chain dehydrogenase/reductase (SDR) family of enzymes. Although the sequence identity within SDR enzymes is quite low (typically 10–30%), two conserved sequence motifs, which are necessary for the maintenance of fold and function, are shared by all of the SDRs [10]. Typically, these enzymes display a similar conserved sequence motif that includes three glycine residues Gly-X-X-X-Gly-X-Gly, that form a turn between a β-strand and an α-helix, and that contact directly the cofactor binding site. Another motif that is present in most of the members of this protein family is the Tyr-X-X-X-Lys motif. This sequence motif is often in the vicinity of a conserved Ser that orients the substrate and that catalyzes the proton transfer to and from reduced and oxidized reaction intermediates. Structure–activity data was derived by site-directed mutagenesis experiments [11] performed on the rat 11βHSD1 that shares an overall 77% sequence identity with the human enzyme, 60% of which concerns the binding site of the enzyme. The rat 11βHSD1 mutants Y179F, Y179S and K183R completely lost enzymatic activity. These results indicate that the residues Tyr179 and Lys183 are directly involved in the catalytic function. The catalytic residues are conserved in the two enzymes and the corresponding residues in the human enzyme Tyr183 and Lys187 belong to the catalytic triad that includes also Ser170. At the 3D structure level, about 30 3D structures of this family have been solved and deposited in the PDB database [12], adopting the conserved nucleotide-binding Rossman fold. Among these SDRs of known structure are the 3β/17β hydroxysteroid dehydrogenase (EC1.1.1.51) [13], 3α/20β hydroxysteroid dehydrogenase (EC 1.1.1.53) [14], tropinone reductase-I (EC1.1.1.236) [15], to cite a few. Due to these available SDR structures, a theoretical 3D structure of 11βHSD1 can be predicted via homology modeling. In 2003, Blum and co-workers [16] developed a theoretical model for the human 11βHSD1 to provide further functional characterization of this enzyme.

Biochemical, genetics and clinical studies suggested that the selective inhibition of 11βHSD1 could offer a therapeutic approach for treating metabolic syndrome and other diseases [17, 18] and the discovery of inhibitors based on experimental high-throughput screening studies have been reported [19, 20]. To the best of our knowledge, however, *in silico* screening for inhibitors based on the 3D structure of 11βHSD1 has not been publicly reported. In this work we report how we were able to identify new inhibitors of the 11βHSD1 enzyme by the methods of computational molecular science. First, the 3D structure of the enzyme was developed via homology modeling, since the 3D structure was not available at the time we started this study. In a second phase, a validation study consisting in the evaluation of the model to discriminate between some selective 11βHSD1 inhibitors from known substrates and non-inhibitor molecules was carried out. Finally, a database containing 114'000 natural molecules was screened by virtual docking, which allowed us to identify food-grade compounds found to bear all structural features necessary for a potent 11βHSD1 inhibitory activity. Since the crystallographic structure of human 11βHSD1 became publicly available in the final stage of our work, the detailed comparison between the crystal

structure and the predicted model was performed and the corresponding structure-based virtual screening experiment based on the crystal structure was also carried out.

Methods

Homology modeling of human 11βHSD1

The amino acids sequence of the human 11βHSD1 (GenBank protein accession number: AAH12593) was downloaded from the NCBI website. Fold recognition was carried out by using the Protein Structure Prediction Meta Server (http://bioinfo.pl/meta/). Typically sharing less than 25% sequence identity with human 11βHSD1, dozens of SDR enzymes of known structure were confidently assigned as homologues by using state-of-the-art fold recognition algorithms (e.g. ORFeus [21], Fugue [22], FFAS [23] and mGenThreader [24]). Among them, the 3β/17β hydroxysteroid dehydrogenase (PDB entry: 1hxh, chain: A, X-ray resolution: 1.2 Å) was found to share the highest statistical scores for sequence-structure compatibility obtained by ORFeus, FFAS and mGenThreader. Therefore, the 1hxhA was selected as the structural template for the homology modeling. Furthermore, the sequence alignment between 11βHSD1 and 1hxhA was generated by profile–profile alignment methods, such as ORFeus, and the 3D model was built by using the WhatIf package [25]. Some four missing loop regions were reconstructed and inserted in the model by using the Biopolymer module of the Sybyl molecular modeling package [26]. The stepwise structure refinement approach for the predicted model was performed with the Sybyl software by using the Tripos atomic force field [26]. The Kollman all-atom charges for protein atoms were used to calculate the electrostatic term, by assigning protonation states at neutral pH to the corresponding amino acids. We used a cut-off set to 12 Å for the non-bonded interactions, and the distance-dependent dielectric model was adopted to roughly mimic the solvent effect. In the first step, we fixed the positions of all of the backbone atoms of the model and performed some 500 steps of Powell minimization on the side chains. In the second step, we removed the constraints over the backbone atoms and the entire protein was minimized for another 1000 steps with a convergence criterion of 0.2 kcal/mol energy change per step.

The 11βHSD1 enzyme is NADPH-dependent, and we considered quite reasonable to include the atomic coordinates of the cofactor NADPH in the final theoretical model. The coordinates of the co-factor could be transferred to our model based on its structural similarity with other proteins from the same family that were found to complex this same cofactor. Therefore, by superimposing the 11βHSD1 model and the similar tropinone reductase-I complex with NADPH (PDB entry: 1ae1), we were able to position in the binding site of our model the 3D model of NADPH ''borrowed'' from the structure 1ae1. The sequence identity between 11βHSD1 and tropinone reductase-I was 25%. We found out that there was no significant van der Waals clashes between protein atoms and NADPH atoms. We did further minimization for the whole structure of the predicted model including the NADPH molecule and this resulted in a very minor conformational change. In a similar way, we have also included in our model the 3D coordinates for the known inhibitor carbenoxolone, ''borrowed'' from the structure of the 3α/20β hydroxysteroid dehydrogenase complex with this compound (PDB Entry: 1hdc). The carbenoxolone location provided the reference binding mode of a typical inhibitor, that was used to assess the quality of the positioning within the binding site of all of the solutions generated during the structure-based virtual screening experiments.

Molecular docking calculations

We used two well-known fixed protein-flexible ligand docking software packages, GOLD [27] and Glide [28] to perform molecular docking calculations on both the modeled and the experimentally derived structures of the 11βHSD1 enzyme. For each docking program, the same binding site was used and three solutions were generated for each ligand. We estimated that the binding site was delimited by all residues falling within a sphere of 10 Å centered on the reference carbenoxolone inhibitor. The binding site of the model was composed out of the following residues: Asn123, Ser170, Leu171, Ala172, Tyr177, Met179, Val180, Tyr183, Lys187, Leu215, Gly216, Leu217, Ile218, Ala250 and Leu251. This binding site also contained the co-factor molecule NADPH.

Concerning the crystallographic structure 1xu9 [29], the binding site residues were selected much in the same way as in the predicted model and included residues Ile121, Thr124, Leu126, Ser170, Leu171, Ala172, Tyr177, Pro178, Met179, Val180, Tyr183, Lys187, Leu215, Gly216, Leu217, Thr222, Ala223, Ala226 and Val227. Since the crystallographic structures are generally refined before they are submitted to the PDB database, we did not carry out any further structure refinement for 1xu9 before it was used for the docking study.

GOLD

GOLD uses a genetic algorithm for the conformational sampling of the ligand. Due to the large database of compounds, the library screening setting values were used. The conformational analysis was carried out for some 1000 genetic algorithm operations on a population size of 50. The operator weights for crossover, mutation and migration were set to the default values of 100, 100 and 0, respectively. Among the available scoring functions, GoldScore [30, 31] was used to rank the generated ligand binding modes. GoldScore is a force field-based scoring function that is made up of four components such as the intermolecular hydrogen bond energy, the ligand torsional strain energy, the intermolecular and the ligand intramolecular van der Waals energy. Optionally, the ligand intramolecular hydrogen bond energy can be added as a fifth parameter. It is possible to customize the empirical parameters but in this work we kept the default values. The GoldScore fitness function has been optimized for binding mode prediction rather than for binding constant estimation.

Glide

Glide is based on a systematic sampling in the conformational space. The conformational sampling procedure is based on a flexible-ligand minimization and on a Monte Carlo sampling. The protein binding site is represented on a grid. The program uses a series of filters to reduce the possible poses of the ligand. The scoring function GlideScore [32] is used to predict relative ligand binding affinities and to rank the proposed binding modes. It is an enhanced version of the ChemScore function [33]. It is a force field-based scoring function that includes additional terms accounting for solvation and repulsive interactions such as steric clash term and buried polar terms for penalizing electrostatic mismatches. The lipophilic–lipophilic term is the same as the one implemented in the original ChemScore function. The hydrogen-bonding term is separated into differently weighted components depending on the charged character of the donor and the acceptor. An additional term penalizes rotatable bonds in the ligand that are restricted in the docked pose and another term rewards instances in which a polar but non-hydrogen-bonding atom is found in a hydrophobic region. We used the standard parameter settings for the calculations.

Molecular dataset designed for the validation of the human 11βHSD1 model

A reference dataset of molecules was compiled that contained 22 11βHSD1 inhibitors, three non-inhibitors and two substrate molecules [20, 34–37]. The non-inhibitor molecules were never reported to possess any inhibitory activity against the enzyme. This dataset was designed after a careful inspection of the available literature using the SciFinder [38] searching interface to the Chemical Abstracts Database.

Natural product dataset for the virtual screening

The dataset that was used for the virtual screening calculation is an in-house database containing 114'000 natural compounds.

Results and discussion

3D models of 11βHSD1

Although structural homologues of human 11βHSD1 can be easily identified by classical sequence based methods (e.g. BLAST), the enzyme shared very low sequence identity ($\leq$25%) with these, implying a remote homology relationship between 11βHSD1 and the templates. Compared to sequence-based methods, the fold recognition methods have generally higher rate of remote homology identification as well as better accuracy for the generated alignment. Profile–profile matching methods were recently developed and were extensively benchmarked [39, 40] to conclude that they have higher alignment accuracy. Instead of using classical sequence alignment methods to

obtain a 3D model, therefore, in our study fold recognition methods were used to select the structural template and to generate the alignment. In a way comparable to sequence identity matching used in selecting the templates, we used the statistical score from fold recognition methods to select the relevant template for the human 11βHSD1. In the present study, the model of the human 11βHSD1 was obtained by selecting the 3β/17β hydroxysteroid dehydrogenase as the template based on an alignment deduced with ORFeus, a profile–profile matching algorithm (Figure 1a). Interestingly enough, the alignment from ORFeus was highly consensual with those generated with some other state-of-the-art fold recognition algorithms (e.g. FFAS & mGenThreader). Although it is not possible to guarantee that 1hxh is the best possible 3D template and that the alignment is the optimal one, we believe that the template selection based on the ORFeus statistical score and the alignment generated by ORFeus were reasonable. Until now, a lots of programs for the building of homology models have been developed (e.g. Modeller [41], Swiss-Model [42], 3D-JIGSAW [43], to cite a few). As remarked by Sali and co-workers [44], the accuracy of the various homology model-building methods is relatively similar when they are used optimally. As in-house we had access to the Whatif software, we used it to build the 3D model of the human 11βHSD1, by suspecting that other model-builders would provide probably a very similar final protein structure. As shown in Figure 1b, the model extended from residues Pro29 to Asn291 and contained a central 6-stranded, all-parallel β-sheet sandwich-like structure, flanked on both sides by 3-helices. The cofactor molecule was positioned in the vicinity of the binding site, according to a procedure previously discussed.

We have used the PROCHECK software [45] to analyze the stereochemical quality of the 11βHSD1 model. The results showed that 92.1% of the residues were in the most favorable regions, whereas only 0.4% residues fell in forbidden regions in the Ramachandran plot. Generally, if the percentage of residues in the most favorable regions is larger than 90%, the stereochemical quality of the protein structure should be regarded as satisfactory. Therefore, the stereochemical quality of the current 11βHSD1 model was judged as being acceptable.

Interestingly, the 3D crystal structure of the human 11βHSD1 enzyme was solved in a final stage of our study. The experimental structure contained the residues in the range Gln21 to Phe289 [29] and it was deposited in the PDB database as entry 1xu9. Almost at the same time, the crystal structure for the guinea pig 11βHSD1 was also determined [46]. Although the crystal structure was just available after we finished our virtual screening experiments, it allowed for a detailed evaluation of the predicted model. We conducted a structural alignment of our model on the experimental structure (1xu9) by using the CE [47] software to obtain an overall RMSD deviation of C^{α} atoms over 223 aligned residues as low as 2.05 Å. In comparison, the average deviation observed between models and experimentally solved structures was reported to be often larger than 3.5 Å, when the sequence identity between a target sequence and a structural template was less than 30% [48]. In fact, the N-terminal fragments ranging from Pro29 to Ala226 were perfectly matched, while a significant structural deviation occurred in the remaining C-terminal part (Figure 1a). The C-terminus of an SDR enzyme contains a flexible region that often changes conformation upon substrate binding to shield the active site from bulky solvent, modulating the enzyme specificity [29]. There is also one motif in the C-terminus of SDR enzymes known to mediate SDR oligomerization [29]. Indeed, that is variable among the members of the SDR superfamily. Using CE structure comparison, we have compared the C-terminal part of 1xu9 ranging from Ala226 to Phe289 against all of the structures of other known SDR enzymes (i.e. all the domains in the c.2.1 superfamily in the SCOP [49] database), and no significant structural neighbor was identified. Therefore, choosing other SDR enzyme structures as template or employing alignment from other algorithms cannot give significant improvement in the quality of the C-terminal model. Moreover, structural neighbor searching was also performed with the C-terminus of 1xu9 against the current PDB database by using CE. Except 11βHSD1 enzyme structures, no other confident structural neighbor could be assigned. We concluded that there was no better template for the C-terminal part in the case when homology modeling was used.

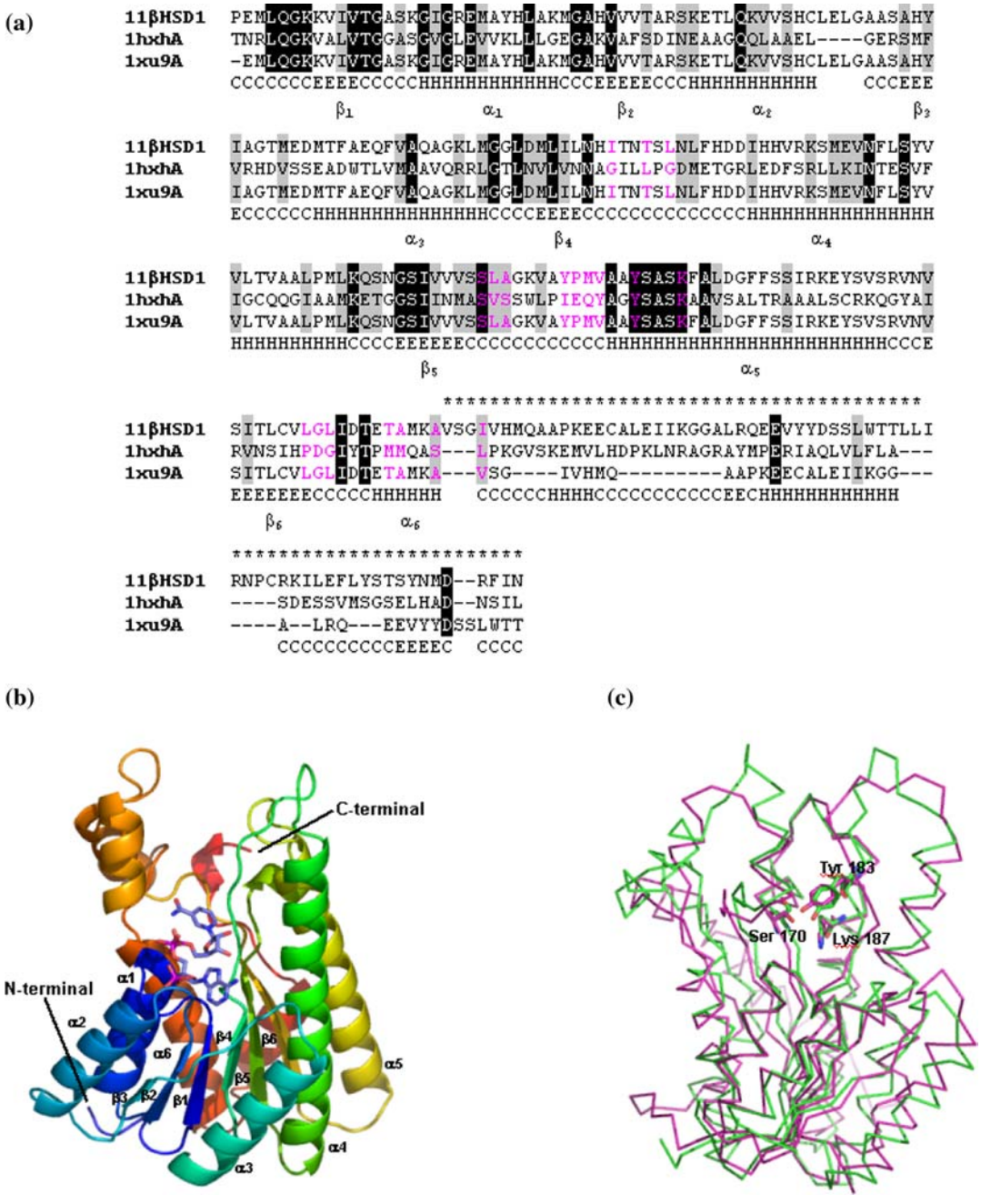

Figure 1. The homology model of human 11βHSD1 from a sequence alignment between human 11βHSD1 and 1hxhA generated with ORFeus. (a) The sequence alignment. To compare the template with the crystal structure, the structure-based sequence alignment between 1hxhA and 1xu9A is also included. The alignment positions with identical amino acids are marked as black blocks, while those with similar amino acids are displayed as gray blocks. The alignment positions labeled as asterisks represent the shift region where the corresponding structure in the theoretical model was not correct. In a fourth line appears the secondary structures of 1hxhA, where "H", "E" and "C" stand for α-helix, β-sheet and random coil, respectively. The α-helices and β-sheets in the correctly predicted region, running from Pro29 to Ala226, are further numbered in a fifth line. Taking the binding site residues assigned from the crystal structure 1xu9A as references, the residues in the corresponding alignment positions are colored in magenta. (b) Cartoon representation of the predicted 3D structure for the human 11βHSD1 containing the cofactor NADPH molecule. (c) Backbone representation of the superimposed structures between the predicted (green) and crystal (magenta) structures of human 11βHSD1. The side-chains for the three catalytic residues (Ser170, Tyr183, Lys187) are displayed as sticks.

We have also performed structural comparison between the crystal structure 1xu9 and the structural template 1hxh. The RMSD for the Cα atoms over 234 residues was 2.34 Å. Since the crystal structure had a slightly larger structural deviation from the homology modeling template than the predicted model, it seems that the current homology modeling method has taken a maximal advantage of the structural template. The RMSD for the Cα atoms between the model and the template was 1.16 Å. In the algorithms nature of homology modeling, the RMSD for the Cα atoms between the model and the template should be close to zero, since the coordinates for atoms of the main chain in template are copied to the homology model. The relatively small deviation between the predicted model and the structural template in the present study could be ascribed to the minor conformational change caused by loop building and energy minimization.

The objective of the homology modeling was to provide a realistic target to carry out docking calculations for the identification of inhibitors. Therefore, it was important to compare the structures of the binding site residues in the theoretical model and the crystal structure. As shown in the structure-based alignment, 18 out of the 19 binding site residues in the crystal structure were well aligned with the corresponding residues in the predicted model (Figure 1a). The CE structural superimposition between the crystal and the predicted structures has shown that the RMSD deviation of the C^{α} atoms over the 19 binding sites residues was 2.21 Å. When taking only the 18 correctly aligned binding site residues into account, the RMSD value decreased to 2.05 Å, much about the same as the overall structural deviation between the model and the crystal structure. Since quite diverse substrate specificities are involved in the SDR enzyme family [29], the active sites for the different SDR enzymes could be more variable than the overall structures. In our model the RMSD in the vicinity of the active site between the predicted model and the experimental structure was slightly larger than the average RMSD value between the overall structures. For more details, the RMSD deviations of the side chain heavy atoms for all these 19 binding site residues after the CE structure alignment have been summarized in Table 1. Generally, these binding site residues were well superimposed, 11 out of the 19 having their side-chain RMSDs less than 3.0Å. In particular, the three catalytic residues Ser170, Tyr183 and Lys187 were perfectly matched with relatively low RMSD deviations for the side-chain heavy atoms (cf. Table 1), a fact that appears also in Figure 1c). We have also evaluated the local side chain conformations by comparing the χ_1 and χ_2 side-chain dihedral angles for these binding site residues in the crystal structure and in the predicted model. We assessed the side chain accuracy of the predicted 11βHSD1 model with the following criteria. For residues that present only one side-chain dihedral angle, the side chain position was considered to be correctly predicted if the χ_1 angle it formed with the corresponding residue in the experimental structure was less than 40°. For residues with more than one dihedral angle in the side-chain, the side chain position was correctly predicted when both χ_1 and χ_2 were within 40°. Since Ala and Gly residues do not have side chain dihedral angles, the local side chain conformation was only evaluated on 15 binding site residues. As also shown in Table 1, five out of 15 residues, including the two catalytic residues Tyr183 and Lys187, could be correctly predicted. We have benchmarked the side chain accuracy for models that were generated with two other methods. In the first method, we copied the C_{α} atoms coordinates from 1hxhA guided by the alignment from ORFeus. Then the backbone and the side chain coordinates were built via the BioPolymer module in the Sybyl package. In the second method, we submitted the ORFeus alignment to the Swiss-Model server (http://swissmodel.expasy.org/) in order to get the homology model. Results showed that the side chain positions for the binding site residues were similar between our 11βHSD1 model and the ones obtained by these two methods. The low quality of these side chains generated with several homology building methods imply that the side-chain modeling still have much space to improve. Finally, we observed that the locations of the cofactor NADPH molecule in the model and the experimental structure were perfectly matching.

The crystallographic study of human 11βHSD1 demonstrated unique tetrameric structure [29]. Each subunit in this complex contained a C-terminal tetramerization motif, a helix-strand-helix conformation, starting at Ser261 and ending at Tyr280. Such a tetramerization motif was not

Table 1. Structural comparison of the binding site residues in the crystal structure and the predicted model.

Residue	RMSD (Å)[a]	χ_1[b]			χ_2[c]		
		$\chi_{1,pred}$	$\chi_{1,1xu9}$	$\lvert\chi_{1,pred} - \chi_{1,1xu9}\rvert$	$\chi_{1,pred}$	$\chi_{1,1xu9}$	$\lvert\chi_{1,pred} - \chi_{1,1xu9}\rvert$
Ile121	2.74	175.7	51.7	124.0	56.2	166.7	110.5
Thr124	3.94	61.6	152.4	90.8	–	–	–
Leu126	8.94	−61.6	−77.5	15.9	75.7	177.0	101.3
Ser170[d]	1.64	180.0	−43.8	136.2	–	–	–
Leu171	2.97	63.3	−69.7	133.0	−55.6	176.8	127.6
Ala172	0.54	–	–	–	–	–	–
Tyr177	0.96	−77.9	−71.1	6.8	71.7	85.9	14.2
Pro178	2.85	−29.4	32.4	61.8	28.3	−37.9	66.2
Met179	3.44	−84.2	−43.2	41.0	−69.7	−50.2	19.5
Val180	2.57	−163.5	−68.7	94.8	–	–	–
Tyr183[d]	0.72	−173.9	170.7	15.4	72.7	87.8	15.1
Lys187[d]	0.38	−72.7	−62.7	10.0	−55.0	−62.4	7.4
Leu215	2.75	44.4	−53.9	98.3	65.3	175.3	110.0
Gly216	1.35	–	–	–	–	–	–
Leu217	3.16	−173.9	175.7	10.4	58.9	64.8	5.9
Thr222	3.06	−168.6	66.0	125.4	–	–	–
Ala223	2.66	–	–	–	–	–	–
Ala226	3.64	–	–	–	–	–	–
Val227	4.50	−58.7	−60.0	1.3	–	–	–

[a]The RMSD deviation of the side-chain heavy atoms (including C^{α} atom) in the predicted model and the crystal structure after the overall CE structure alignment.
[b]The first side-chain dihedral angle.
[c]The second side-chain dihedral angle.
[d]Active site residue.

observed in the template (1hxh) or in other SDR enzymes. This led to a low quality model for the C-terminal part of the 11βHSD1, and therefore, it was not possible to predict the multimeric structure of the human 11βHSD1 by relying only on homology modeling. This has not affected our objective of identifying new inhibitors based on molecular docking studies using structural information concerning the inhibitor binding site. We suspect however that the current model of the enzyme would be of limited use for predicting subunit assembly by further computational studies, such as protein–protein docking [50].

In our work we tried to address an important topic in current post-genomic computational science related to the understanding of molecular recognition properties of one protein, based on the knowledge about the 3D structure of its closest homologue. In a recent contribution Zhang and Skolnick [51] examined the "structural" completeness of the version of the Protein Data Bank (PDB) in 2004. The authors found that the protein-folding problem can in principle be solved for practically any sequence based on this version of the PDB library provided that efficient fold recognition algorithms can recover correct sequence alignments. Our results were encouraging in the fact that the structural model of the investigated protein, human 11βHSD1, and the experimentally determined structure were found to be very close. We concluded therefore that the model of the human 11βHSD1 enzyme that we derived via homology modeling was sufficiently accurate to be used in molecular docking experiments. Although the crystal structure was just released, we performed docking calculations by using it, which will be further discussed in the following section.

Validation of the model

The validation of the 11βHSD1 model consisted in evaluating its ability to discriminate 11βHSD1 inhibitor molecules from substrates and inactive

compounds. To reach this goal, we performed structure-based virtual screening calculations with a reference database. This database was constituted of 27 molecules with experimentally determined activities towards 11βHSD1. GOLD and Glide software packages were used to perform virtual screening calculations. For each docking program, the same binding site was used and three solutions were generated for each ligand. In order to further evaluate the accuracy and the quality of our model, molecular docking calculations with the reference dataset was applied in parallel on the crystallographic structure of 11βHSD1 with the Glide program. The results obtained for both targets for the energy top-ranked binding modes are reported in Table 2. GOLD and Glide docking programs were described in comparative studies to give good docking accuracies [52–56]. In the present study, the two programs were used for the purpose of ligand binding mode comparison. We used the performance and the advantages of both docking tools in a consensual way in order to get a better confidence on the generated and proposed results. GOLD is a faster docking program compared to Glide. In another aspect, the scoring function implemented in Glide was described to be especially effective for database screening. Within the context of virtual screening calculations, we decided to run a first screening with GOLD in order to decrease the number of molecules for more accurate screening with Glide. Regarding the Glide results, it appeared that the

Table 2. Results of the virtual screening calculations of the reference database used to validate the 11βHSD1 model.

Ligand	Activity	Model		1xu9
		GoldScore[a]	GlideScore[b]	GlideScore[b]
TZD 2	Inhibitor	55.98	−11.29	−8.55
Saquinavir	Inhibitor	49.47	−9.98	−7.86
Indinavir	Inhibitor	14.50	−9.05	−8.10
Rosiglitazone	Inhibitor	41.22	−8.33	−7.34
BVT 14225	Inhibitor	16.51	−8.02	−7.32
BVT2733	Inhibitor	16.38	−7.96	−6.76
Benzenesulfonamide	Inhibitor	21.92	−7.86	−6.47
Cyclobutanone	Inhibitor	32.91	−7.38	−7.68
4′-Hydroxyflavanone	Inhibitor	47.27	−7.23	−6.62
1-Piperidinecarboxylic acid	Inhibitor	5.65	−7.15	−7.60
11-Ketotestosterone	Inhibitor	37.63	−7.14	−7.43
Chenodeoxycholic acid	Inhibitor	20.20	−6.85	−6.92
NSC 112288	Inhibitor	26.80	−6.83	−7.45
DETC	Non inhibitor	10.02	−6.81	−5.54
Flavanone	Inhibitor	46.57	−6.77	−6.03
Flavone	Non inhibitor	43.33	−6.72	−6.04
2′-Hydroxyflavanone	Inhibitor	39.58	−6.62	−5.83
Abietic acid	Weak inhibitor	24.55	−6.24	−6.83
Ethanone	Inhibitor	51.62	−6.24	−5.64
Bisphenol A	Non inhibitor	26.78	−6.22	−5.60
Cortisone	Substrate	19.80	−6.17	−6.97
NSC 75617	Inhibitor	27.88	−5.78	−7.75
Dihydroxy-5a-androstan-11-one	Inhibitor	23.85	−5.70	−7.45
NSC 56412	Inhibitor	26.91	−5.53	−7.53
15-Deoxy-D12,14-PGJ2	Substrate	29.13	−5.42	−5.95
Methyljasmonate	Weak inhibitor	33.23	−4.36	−4.16
Resorcinol	Weak inhibitor	31.10	−3.49	−3.45

[a]GOLD energy units.
[b]Glide energy units.

selective 11βHSD1 inhibitors bind to the enzyme model with energies, approximated by the respective GlideScore values, that were lower than −7.00 (arbitrary units used in Glide). Concerning GOLD, the inhibitors had a GoldScore values greater than 46 (arbitrary units in GOLD). With these two energy cut-offs we were able to retrieve five inhibitors out of the 22 from the reference dataset. Our model allowed to discriminate between selective inhibitors, non-inhibitors and substrate molecules, and this gave us good confidence that it can be further used in exploratory virtual screening experiments to identify putative selective 11βHSD1 inhibitors in large databases of compounds. Concerning the generated binding modes, for 32% of the enzyme inhibitors, both docking programs GOLD and Glide predicted poses that shared RMSD values lower than 3 Å.

Interestingly, we compared the predicted binding modes docked with our model with the ones obtained with the 3D 11βHSD1 crystallographic structure. To be concise we will discuss only the Glide results here. It appeared that the binding modes obtained for each enzyme structure and each ligand were relatively close (Figure 2). As the two protein models had a RMSD of nearly 2 Å, we were not able to calculate pair-wise RMSD values between pairs of solutions. The generation of similar binding modes derived from both the experimental structure and the homology model of the enzyme indicate that the virtual screening results could be considered as consensual.

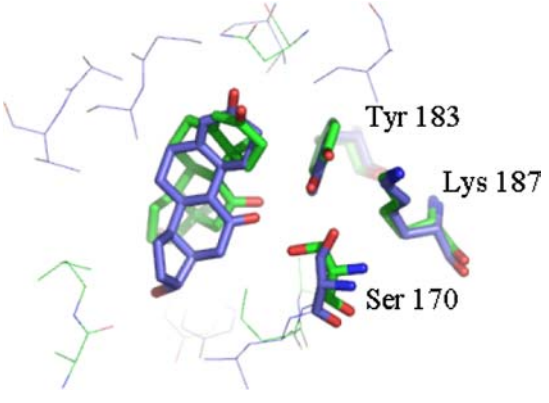

Figure 2. Comparison of the binding modes of the 11βHSD1 inhibitor 11-ketotestosterone proposed based on the 11βHSD1 model (green) and the 3D crystallographic structure (purple). Binding modes were generated by the Glide docking software.

Probably, the most important conclusion from our work was that the relatively crude homology model was able to predict binding modes that were reproduced with an experimental structure.

On the other hand, we investigated the correlation between the binding energies and ligand affinities derived with the two enzyme structures. We used the GlideScore scoring function to calculate these energies. The GlideScore values for each ligand of the reference dataset are reported in Figure 3, and the correlation coefficient R reached the value of 0.69. In conclusion we estimated that the derived homology model gave results that were geometrically and energetically comparable to the ones obtained based on the experimentally solved structure. This strengthened our confidence in the quality of the model and on its usefulness to perform *in silico* screening for the identification of human 11βHSD1 inhibitors.

Inhibitory binding mode

The inhibition of 11βHSD1 activity results from the direct competition with the substrate for binding [29]. Catalytic residues Ser170, Tyr183 and Lys187 appear to maintain the inhibitor in a fixed position relative to the cofactor position, while the substrate-binding pocket fails to accommodate substrates in which the cortisone keto-group to be reduced is brought into bonding distance to the Tyr183 hydroxyl. Therefore, inhibitors must form strong hydrogen bonds to one or more amino acid residues directly involved in catalysis in order to displace the substrate and/or the cofactor. Most of the 11βHSD1 inhibitors present a carbonyl or thiocarbonyl oxygen atom able to form hydrogen bonds with the catalytic residues Ser170 and/or Tyr183. As the steroid-binding site is highly hydrophobic, the rest of the molecule makes with the protein some stabilizing hydrophobic interactions. Binding modes obtained for the cortisone (substrate) and the benzenesulfonamide (inhibitor) molecules are shown in Figure 4. The strength of the interaction between a ligand and a receptor is estimated through a scoring function value that is assigned to the predicted binding mode. From the molecular docking calculation, it can be deduced that the benzenesulfonamide molecule makes a stronger interaction with the binding site residues of the enzyme than the cortisone endogenous substrate

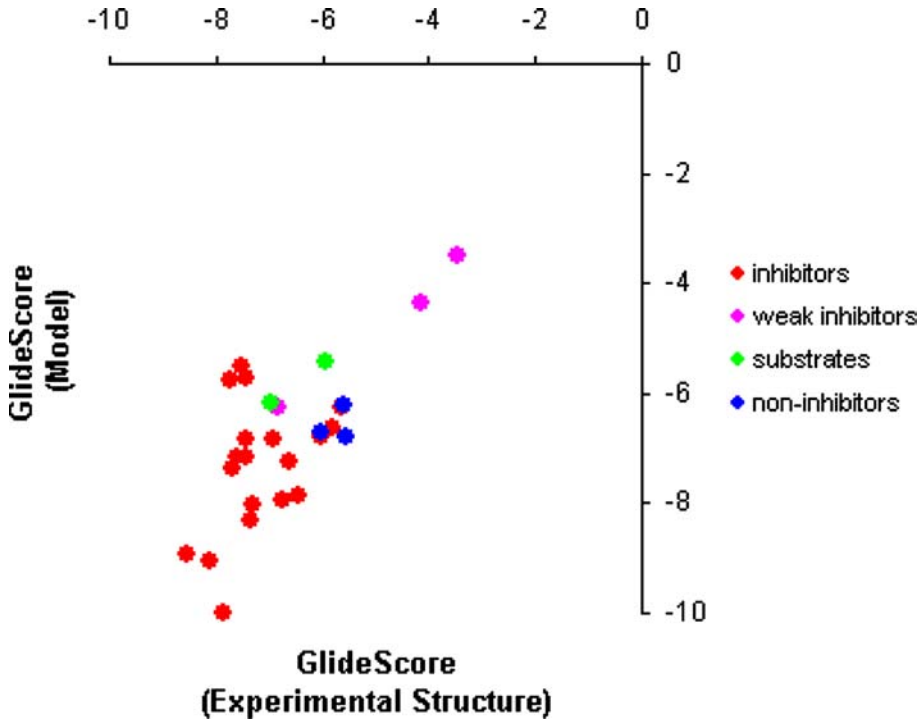

Figure 3. Correlation between the GlideScore values for every molecule of the reference dataset. The binding modes were predicted using the 11βHSD1 model and the crystallographic structure 1xu9 as receptors. The correlation factor R is 0.69 and 0.71 for the overall reference dataset and the known inhibitors, respectively.

as their respective GlideScore values were −7.86 and −6.17 (glide energy units).

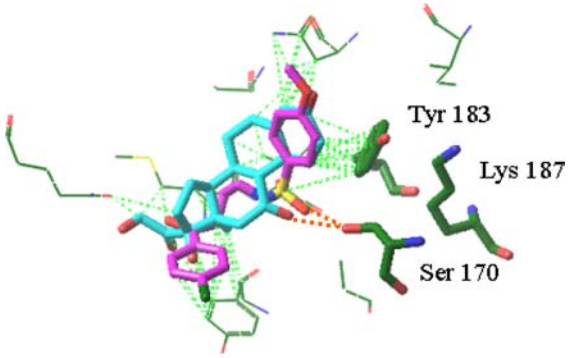

Figure 4. Binding modes of the endogenous substrate cortisone (blue) and the benzenesulfonamide inhibitor molecule (pink) within the 11βHSD1 model. Binding modes were generated by the Glide docking software with the respective GlideScore scoring function values of −6.17 and −7.86 (Glide energy units). Orange dashed lines represent intramolecular hydrogen bonds. Green dashed lines represent stabilizing hydrophobic contacts.

Virtual screening of the database of natural molecules

The validation of our model of the human 11βHSD1 confirmed that it could be used like the crystallographic structure in *in silico* screening experiments aimed at identifying new selective inhibitors of the enzyme. A database containing 114'000 natural molecules was used to perform virtual docking calculations. In order to obtain a meaningful comparison, the first virtual screening of the database was carried out on both receptors: the model and the crystallographic structure. The initial full screening of the database was carried out with the fast GOLD program by setting the default virtual screening parameters. For each ligand, only the top-scoring binding mode was generated. After the calculation, the molecules were sorted according to their GoldScore values. Consequently, we applied the numerical cut-off of 46 GOLD energy units, discussed previously, to select all potential inhibitors. By this filter, we obtained 2736 molecules for the receptor model

and 3705 molecules for the crystallographic structure. A second virtual screening calculation using the Glide program with the GlideScore function was carried out on these molecules. In order to get consensus solutions, calculations were performed both on our model and on the crystallographic structure of the 11βHSD1 enzyme. The same calculation parameters were set up for both the model and the experimentally solved binding sites. One solution was generated for each ligand. We obtained 70 solutions using the 11βHSD1 model and 74 solutions with the crystallographic structure 1xu9 that docked in the respective binding sites. Of the 70 solutions identified with our model, 29 passed the GlideScore energy filter of −7.00 Glide energy units, while only 18 were selected based on the experimental structure. Further, we found out that the two sub-selections based on our model and on the recently published experimental structure were consensual over 15 molecules, which represented 50% of the solutions found with the model and nearly 84% of the solutions identified with the experimental structure. As we indicated previously it was not possible to derive pair-wise RMSD values for the consensual solutions due to the slight deviations between the model and experimental structures. However, the visual inspection of the consensual binding modes for a given molecule revealed that they are relatively close. Furthermore, a high degree of superimposition was observed in the binding modes of the known inhibitors and the ones identified by our *in silico* screening experiments. As an example this superimposition is displayed in Figure 5. The predicted binding modes of the known 11βHSD1 inhibitor flavanone and of one of our proposed molecules (NRD10012) are represented docked within the enzyme model and within the experimentally determined structure. In each structure, the binding mode of the inhibitor and the proposed one are consensual, i.e. both molecules share similar interactions with the key binding site residues. As we did it in the model validation phase of our work, we calculated the correlation of the GlideScore values between the solutions obtained for both targets (Figure 6). The calculated correlation factor R for the 15 putative inhibitors was 0.71, which is the same value that was found for the known inhibitors of the reference dataset. As expected, the selected molecules formed hydrogen bonds with at least one of the catalytic residues Ser170 or Tyr183. All of the tentative inhibitors possess a hydrophobic and planar core that can form stabilizing contacts with the hydrophobic residues of the binding site such as Ile121, Leu123, Met179, Val180, Tyr183 and Ile218. Aromatic groups were contributing to the stabilization of the complex through π–π stacking interactions with Tyr183. The hits are reported in Table 3. As *in vitro* screening assays will be performed to validate the inhibition of the reductase activity of the proposed compounds, we are not able at the moment to disclose all of their structures. However, it can be mentioned that

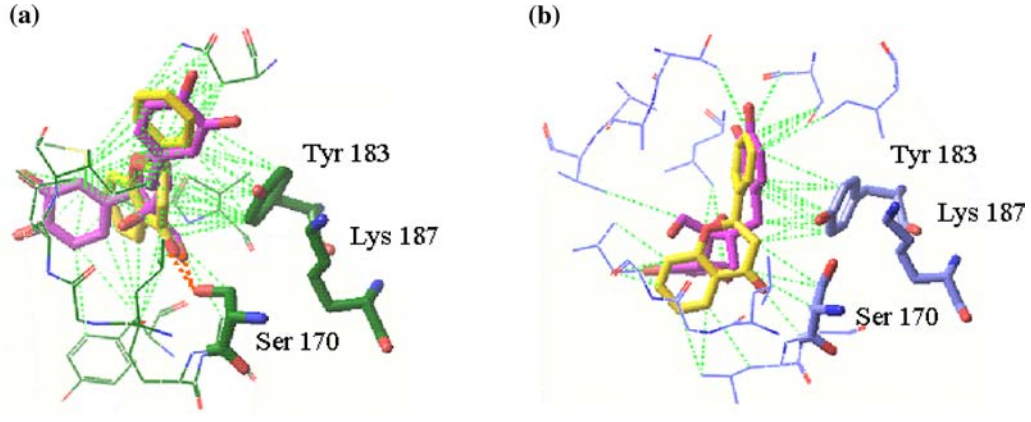

Figure 5. Binding modes of the inhibitor molecule flavanone (yellow) and a suggested 11βHSD1 inhibitor molecule named NRD10012 (pink). Binding modes where docked (a) within the 11βHSD1 model and (b) within the experimental structure of the 11βHSD1 enzyme. Orange dashed lines represent intramolecular hydrogen bonds. Green dashed lines represent stabilizing hydrophobic contacts.

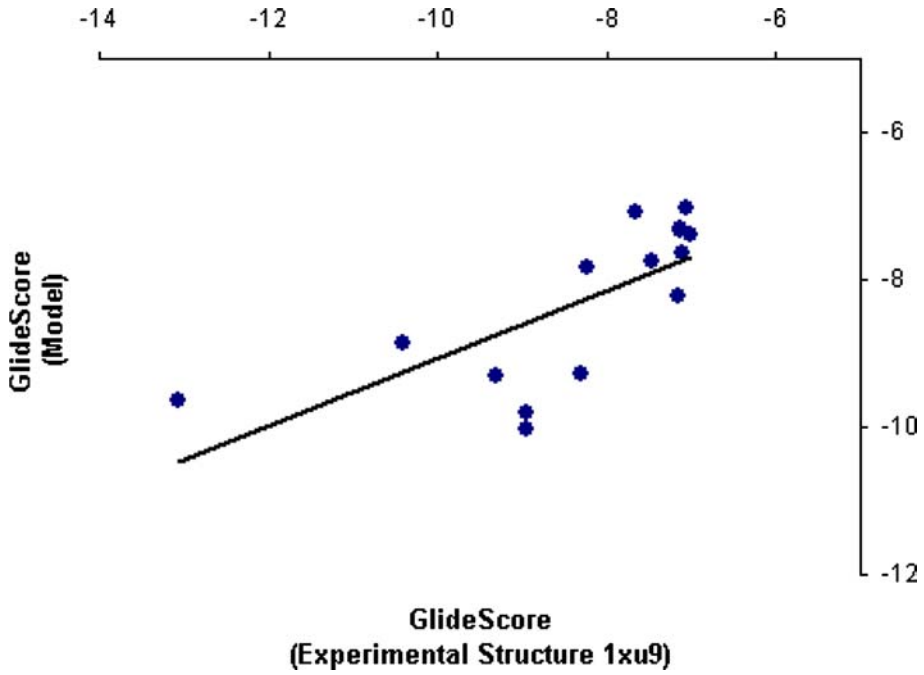

Figure 6. Correlation between the GlideScore values for the 15 proposed 11βHSD1 inhibitors. The binding modes were predicted using the 11βHSD1 model and the crystallographic structure 1xu9 as receptors. The correlation factor R is 0.71.

some of these structures cover several flavonoid classes. Among them, two flavanone derivatives were selected by our structure-based molecular docking calculations. These compounds are NRD100011 and NRD100014. A previous screening assay on 11βHSD1-transfected cells demonstrated

Table 3. Virtual screening results for 15 putative human selective 11βHSD1 inhibitors found in a consensus way from the *in silico* screenings carried out on the 11βHSD1 model and on the experimental structure (1xu9) of the enzyme.

Name	Lipinski Number[a]	Model		1xu9
		GoldScore[b]	GlideScore[c]	GlideScore[c]
NRD10001	1	68.29	−9.63	−13.06
NRD10002	4	66.93	−8.86	−10.40
NRD10003	4	64.68	−9.31	−9.30
NRD10004	1	60.73	−9.81	−8.96
NRD10005	4	64.75	−10.03	−8.95
NRD10006	3	59.89	−9.28	−8.31
NRD10007	3	58.57	−7.83	−8.22
NRD10008	5	47.37	−7.08	−7.65
NRD10009	5	48.88	−7.76	−7.46
NRD10010	4	47.34	−8.23	−7.16
NRD10011	5	63.07	−7.33	−7.13
NRD10012	4	69.36	−7.31	−7.12
NRD10013	5	64.02	−7.65	−7.11
NRD10014	5	61.51	−7.03	−7.07
NRD10015	5	47.32	−7.40	−7.02

[a]The Lipinski Number represents the number of the Lipinski criteria met by the given compound.
[b]GOLD energy units.
[c]Glide energy units.

that flavanone selectively inhibited this enzyme [20]. In particular, flavanone and 2′-hydroxyflavanone efficiently inhibited the enzyme activity with respective IC_{50} values of 18 and 10 μM. This result reinforced our confidence in the quality of our structure-based approach.

In order to estimate the drug-likeness of the selected compound, the values of the respective Lipinski's rule molecular properties were calculated. The Lipinski "Rule of Five" [57] states that compounds are likely to have good absorption and permeation in biological systems and are more likely to be successful drug candidates if they meet the following criteria: the candidate compound should have five or fewer hydrogen-bond donors, ten or fewer hydrogen-bond acceptors, a molecular weight less than or equal to 500, a calculated log *P* less than or equal to 5 and a number of rotatable bonds less or equal to 10. The values for these molecular properties for the 15 candidate molecules are reported in Table 3. Among the 15 proposed candidates, six matched perfectly the different criteria that make them the ideal candidates for forthcoming biochemical experiments.

Conclusions

11βHSD1 inhibition is a promising target for the treatment of a host of human disorders that might benefit from blockade of glucocorticoid action, such as obesity, metabolic syndrome, diabetes type 2. The goal of our study was to identify new putative selective human 11βHSD1 inhibitors by using the methods of computational molecular science. As no experimental structure of the enzyme was solved when we started the study, we employed homology modeling to build the 3D structure of 11βHSD1. Molecular docking was used to validate the model showing that it was able to discriminate 11βHSD1 inhibitors from a reference dataset composed of molecules with known activities towards this enzyme target. Arriving in the final stages of the work, a crystal structure for the enzyme became publicly available. The binding modes inferred with the docking calculations on both the 11βHSD1 model and the experimental structure of the 11βHSD1 enzyme were found to be geometrically and energetically similar. Based on this *in silico* screening study 15 putative new 11βHSD1 inhibitor molecules were proposed, that met all drug-likeness criteria, and will be considered in forthcoming biochemical experiments.

Acknowledgements

We thank Dr. Catherine Mace and Dr. Christian Darimont for bringing to our attention the importance of the subject as well as for the numerous discussions we had on the topic. We thank also both reviewers for their constructive comments and suggestions that helped us to improve the quality of our work.

References

1. Bjorntorp, P. and Obesity, , Lancet, 350 (1997) 423.
2. Zimmet, P., Alberti, K.G. and Shaw, J., Nature, 414 (2001) 782.
3. Ricketts, M.L., Shoesmith, K.J., Hewison, M., Strain, A., Eggo, M.C. and Stewart, P.M., J. Endocrinol., 156 (1998) 159.
4. Tomlinson, J.W., Walker, E.A., Bujalska, I.J., Draper, N., Lavery, G.G., Cooper, M.S., Hewison, M. and Stewart, P.M., Endocrine Rev., 25 (2004) 831.
5. Agarwal, A.K., Monder, C., Eckstein, B. and White, P.C., J. Biol. Chem., 264 (1989) 18939.
6. Engeli, S., Bohnke, J., Feldpausch, M., Gorzelniak, K., Heintze, U., Janke, J., Luft, F.C. and Sharma, A.M., Obes. Res., 12 (2004) 9.
7. Masuzaki, H., Paterson, J., Shinyama, H., Morton, N.M., Mullins, J.J., Seckl, J.R. and Flier, J.S., Science, 294 (2001) 2166.
8. Kotelevtsev, Y., Holmes, M.C., Burchell, A., Houston, P.M., Schmoll, D., Jamieson, P., Best, R., Brown, R., Edwards, C.R., Seckl, J.R. and Mullins, J.J., Proc. Natl. Acad. Sci. USA, 94 (1997) 14924.
9. Morton, N.M., Holmes, M.C., Fievet, C., Staels, B., Tailleux, A., Mullins, J.J. and Seckl, J.R., J. Biol. Chem., 276 (2001) 41293.
10. Agarwal, A.K., Rogerson, F.M., Mune, T. and White, P.C., Genomics, 29 (1995) 195.
11. Obeid, J. and White, P.C., Biochem. Biophys. Res. Commun., 188 (1992) 222.
12. Berman, H.M., Westbrook, J., Feng, Z., Gilliland, G., Bhat, T.N., Weissig, H., Shindyalov, I.N. and Bourne, P.E., Nucleic Acids Res., 28 (2000) 235.
13. Benach, J., Filling, C., Oppermann, U.C., Roversi, P., Bricogne, G., Berndt, K.D., Jornvall, H. and Ladenstein, R., Biochemistry, 41 (2002) 14659.
14. Ghosh, D., Erman, M., Wawrzak, Z., Duax, W.L. and Pangborn, W., Structure, 2 (1994) 973–980.
15. Nakajima, K., Yamashita, A., Akama, H., Nakatsu, T., Kato, H., Hashimoto, T., Oda, J. and Yamada, Y., Proc. Natl. Acad. Sci. USA, 95 (1998) 4876.
16. Blum, A., Raum, A. and Maser, E., Biochemistry, 42 (2003) 4108.

17. Moore, J.S., Monson, J.P., Kaltsas, G., Putignano, P., Wood, P.J., Sheppard, M.C., Besser, G.M., Taylor, N.F. and Stewart, P.M., J. Clin. Endocrinol. Metab., 84 (1999) 4172.
18. Morton, N.M., Paterson, J.M., Masuzaki, H., Holmes, M.C., Staels, B., Fievet, C., Walker, B.R., Flier, J.S., Mullins, J.J. and Seckl, J.R., Diabetes, 53 (2004) 931.
19. Barf, T., Vallgarda, J., Emond, R., Haggstrom, C., Kurz, G., Nygren, A., Larwood, V., Mosialou, E., Axelsson, K., Olsson, R., Engblom, L., Edling, N., Ronquist-Nii, Y., Ohman, B., Alberts, P. and Abrahmsen, L., J. Med. Chem., 45 (2002) 3813.
20. Schweizer, R.A.S., Atanasov, A.G., Frey, B.M. and Odermatt, A., Molecular and Cellular Endocrinology, 212 (2003) 41.
21. Ginalski, K., Pas, J., Wyrwicz, L.S., von Grotthuss, M., Bujnicki, J.M. and Rychlewski, L, Nucleic Acids Res., 31 (2003) 3804.
22. Shi, J., Blundell, T.L. and Mizuguchi, K., J. Mol. Biol., 310 (2001) 243.
23. Rychlewski, L., Jaroszewski, L., Li, W. and Godzik, A., Protein Sci., 9 (2000) 232.
24. McGuffin, L.J. and Jones, D.T., Bioinformatics, 19 (2003) 874.
25. Vriend, G., J. Mol. Graph., 8 (1990) 52.
26. Sybyl, Version 7.0, Tripos Inc, St. Louis, MO, 2004.
27. GOLD, Version 2.1, CCDC Software Limited, Cambridge, 2003.
28. Glide, Version 3.5, Schrödinger Inc, Portland, 2004.
29. Hosfield, D.J., Wu, Y., Skene, R.J., Hilgers, M., Jennings, A., Snell, G.P. and Aertgeerts, K., J. Biol. Chem., 280 (2005) 4639.
30. Jones, G., Willett, P. and Glen, R.C., J. Mol. Biol., 245 (1995) 43.
31. Jones, G., Willett, P., Glen, R.C., Leach, A.R. and Taylor, A.R., J. Mol. Biol., 267 (1997) 727.
32. Friesner, R.A., Banks, J.L., Murphy, R.B., Halgren, T.A., Klicic, J.J., Mainz, D.T., Repasky, M.P., Knoll, E.H., Shelley, M., Perry, J.K., Shaw, D.E., Francis, P. and Shenkin, P.S., J. Med. Chem., 47 (2004) 1739.
33. Eldridge, M.D., Murray, C.W., Auton, T.R., Paolini, G.V. and Mee, R.P., J. Comput-Aided Mol. Des., 11 (1997) 425.
34. Berger, J., Tanen, M., Elbrecht, A., Hermanowski-Vosatka, A., Moller, D.E., Wright, S.D. and Thieringer, R., J. Biol. Chem., 276 (2001) 12629.
35. Barton, P.J., Clarke, D.S., Davies, C.D., Hargreaves, R.B., Pease, J.E. and Rankine, M.T., PCT Int. Appl. WO 2004011410, 2004.
36. Morris, D.J. and Brem, A.S., PCT Int. Appl. WO 2003059267, 2003.
37. Olson, S.H., Balkovec, J.M. and Zhu, Y., PCT Int. Appl. WO 2003059267, 2003.
38. SciFinder, 2004 Edition, American Chemical Society, 2004.
39. Ohlson, T., Bjorn, W. and Elofsson, A., Proteins, 57 (2004) 188.
40. Zhang, Z., Kochhar, S. and Grigorov, M.G., Protein Sci., 14 (2005) 431.
41. Sali, A. and Blundell, T.L., J. Mol. Biol., 234 (1993) 779.
42. Schwede, T., Kopp, J., Guex, N. and Peitsch, M.C., Nuclei Acids Res., 31 (2003) 3381.
43. Bates, P.A., Kelley, L.A., MacCallum, R.M. and Sternberg, M.J.E., Proteins, Suppl 5 (2001) 39.
44. Marti-Renom, M.A., Stuart, A., Fiser, A., Sanchez, R., Melo, F. and Sali, A., Annu. Rev. Biophys. Biomol. Struct., 29 (2000) 219.
45. Laskowski, R.A., MacArthur, M.W., Moss, D.S. and Thornton, J.M., J. Appl. Cryst., 26 (1993) 283.
46. Ogg, D., Elleby, B., Norstrom, C., Stefansson, K., Abrahmsen, L., Oppermann, U. and Svensson, S., J. Biol. Chem., 280 (2004) 3789.
47. Shindyalov, I.N. and Bourne, P.E., Protein Eng., 11 (1998) 739.
48. Kopp, J. and Schwede, T., Pharmacogenomics, 5 (2004) 405.
49. Murzin, A.G., Brenner, S.E., Hubbard, T. and Chothia, C., J. Mol. Biol., 247 (1995) 536.
50. Russell, R.B., Alber, F., Aloy, P., Davis, F.P., Korkin, D., Pichaud, M., Topf, M. and Sali, A., Curr. Opin. Struct. Biol., 14 (2004) 313.
51. Zhang, Y. and Skolnick, J., Proc. Natl. Acad. Sci. USA, 102 (2005) 1029.
52. Kellenberger, E., Rodrigo, J., Muller, P. and Rognan, D., Proteins, 57 (2004) 225.
53. Perola, E., Walters, W.P. and Charifson, P.S., Proteins, 56 (2004) 235.
54. Krovat, E.M., Steindl, T. and Langer, T., Comp. Aided Drug Des., 1 (2005) 93.
55. Friesner, R.A., Banks, J.L., Murphy, R.B., Halgren, T.A., Klicic, J.J., Mainz, D.T., Repasky, M.P., Knoll, E.H., Shelley, M., Perry, J.K., Shaw, D.E., Francis, P. and Shenkin, P.S., J. Med. Chem., 47 (2004) 1739.
56. Halgren, T.A., Murphy, R.B., Friesner, R.A., Beard, H.S., Frye, L.L., Pollard, W.T. and Banks, J.L., J. Med. Chem., 47 (2004) 1750.
57. Lipinski, C.A., J. Pharm. Toxicol. Meth., 44 (2001) 235.